Luteinizing hormone stimulates ingression of granulosa cells within the mouse preovulatory follicle.

Corie M. Owen and Laurinda A. Jaffe

Department of Cell Biology, University of Connecticut Health Center, Farmington, CT 06030 USA

*Authors for correspondence (coowen@uchc.edu, ljaffe@uchc.edu)

RUNNING TITLE: Granulosa cell ingression

KEY WORDS: Ovarian follicle, luteinizing hormone receptor, granulosa cell, ingression, ovulation, mouse

SUMMARY STATEMENT: In response to luteinizing hormone, granulosa cells expressing its receptor elongate into the mouse ovarian follicle interior; the ingression may contribute to changes in follicular structure that enable ovulation.

ABSTRACT

Luteinizing hormone (LH) induces ovulation by initiating signaling by the mural granulosa cells that surround a mammalian oocyte in an ovarian follicle. However, much remains unknown about how LH activation of its receptor (LHR) modifies the structure of the follicle such that the oocyte is released and the follicle remnants are transformed into the corpus luteum. The present study shows that the preovulatory surge of LH stimulates LHR-expressing granulosa cells, initially located almost entirely in the outer layers of the mural granulosa, to rapidly extend inwards, intercalating between other cells. The proportion of LHR-expressing cell bodies in the inner half of the mural wall increases until the time of ovulation, with no change in the total number of cells expressing the receptor. Many of the initially flask-shaped cells appear to detach from the basal lamina, acquiring a rounder shape with multiple filipodia. Following the ingression of the LHR-expressing cells, but still hours before ovulation, the follicular wall develops numerous invaginations and constrictions. LH stimulation of granulosa cell ingression may contribute to changes in the follicular structure that enable ovulation.

INTRODUCTION

Mammalian oocytes are maintained and grow within ovarian follicles, structures comprised of many concentric layers of somatic cells. Directly around the oocyte are cumulus cells, and outside of these are mural granulosa cells, a basal lamina, and a theca layer including steroidogenic cells, fibroblasts, smooth muscle cells, and vasculature (Richards et al., 2018) (Figure 1A). During each reproductive cycle, granulosa cells of preovulatory follicles start to express receptors for luteinizing hormone (LH) (Baena et al., 2020; Bortolussi et al., 1979; Uilenbroek and Richards, 1979), which is released from the pituitary to stimulate ovulation. The LH receptor (LHR) is expressed on a subset of the outer granulosa cells, as well as some theca cells (Baena et al., 2020; Bortolussi et al., 1977; Bortolussi et al., 1979; Eppig et al., 2002; Peng et al., 1991; Richards et al., 1976; Uilenbroek and Richards, 1979). Binding of LH to its receptor induces meiotic resumption in the oocyte and changes in gene expression in the granulosa cells, via a G-protein-coupled signaling cascade (Das and Arur, 2022; Duffy et al., 2019; Hughes and Murphy, 2021; Jaffe and Egbert, 2017; Liu et al., 2014; Richards and Ascoli, 2018; Sposini and Hanyaloglu, 2018).

Activation of the LHR also causes complex structural changes in the follicle. These include chromosomal and cytoskeletal rearrangements as meiosis progresses in the oocyte (Harasimov et al., 2023), secretion of an extracellular matrix from the cumulus cells and loss of connections between these cells and the oocyte (Clarke, 2022; Eppig, 1982), and thinning of the mural granulosa and theca layers at the apex where ovulation will occur (Downs and Longo, 1983; Lipner and Cross, 1968; Martin and Talbot, 1987; Migone et al., 2016). The thinning of the apical layers is correlated with vasoconstriction and reduced blood flow in the apical region of the theca (Migone et al., 2016). At the time of ovulation, the basal lamina around the granulosa cells breaks down and blood vessels from the theca grow inwards as the remnants of the follicle transform into the corpus luteum, which produces progesterone to support pregnancy (Stocco et al., 2007).

As ovulation approaches, the mural granulosa and theca layers in the basal lateral region of the follicle develop constrictions, and these are thought to contribute to expelling the oocyte and surrounding cumulus cells (Brown et al., 2010; Gothié, 1967; Ko et al., 2006; Martin and Talbot, 1981; Szołtys et al., 1994; Talbot and Chacon, 1982). The preovulatory constrictions may be mediated in part by contraction of smooth muscle cells in the overlying theca (Martin and Talbot, 1981), in response to endothelin-2 produced by the granulosa cells (Ko et al., 2006;

Ko et al., 2022; Palanisamy et al., 2006). However, granulosa-specific deletion of endothelin-2 in mice only partially inhibits ovulation (Cacioppo et al., 2017), indicating that additional factors may contribute to the follicular constriction.

One such factor is suggested by evidence that LH induces migration (Bianco et al., 2019; Grossman et al., 2015) and shape changes (Ben-Ze'ev and Amsterdam, 1989; Karlsson et al., 2010) in isolated granulosa cells. Since cell migration and shape changes can regulate tissue architecture in other developmental systems (Lecuit and Lenne, 2007; Walck-Shannon and Hardin, 2014), including the *Drosophila* ovarian follicle (Parsons et al., 2023), we examined whether LH stimulates cell motility in LHR-expressing granulosa cells within ovarian follicles.

By collecting ovaries for imaging at designated times after a physiological LH stimulus, we obtained a precise timecourse of changes in LHR localization over the period leading to ovulation. We discovered that LH stimulates granulosa cells that express its receptor to extend inwards in the follicle, intercalating between other granulosa cells. This LH-stimulated granulosa cell motility may influence the structure of the follicle as it prepares for ovulation and transformation into a corpus luteum.

RESULTS AND DISCUSSION

LH release was stimulated by intraperitoneal injection of kisspeptin (Owen et al., 2021), a neuropeptide that causes gonadotropin releasing hormone to be secreted from the hypothalamus, which in turn causes release of LH into the bloodstream (Stevenson et al., 2022). The rise in serum LH peaks ~1.5 hours after kisspeptin injection and is comparable in amplitude and duration to the endogenous LH surge (Owen et al., 2021).

With the experimental conditions used here, ovulation occurred between 11 and 12 hours after injection of mice with kisspeptin (Figure 1B). The timing and number of oocytes released were similar comparing HA-LHR and wild-type mice, and similar comparing kisspeptin and human chorionic gonadotropin (hCG), which is commonly used to stimulate ovulation (Figure 1B). Based on these kinetics, ovaries from HA-LHR mice were collected, fixed, and frozen, either before kisspeptin injection, or at 2 hour intervals afterwards (Figure 1C). Ovary cryosections were then labelled with an HA antibody, and the localization of HA-LHR expressing cells was analyzed.

LH induces inward extension of LHR-expressing granulosa cells within the preovulatory follicle

The localization of cells expressing the LHR was investigated after a physiological LH stimulus, using a recently developed mouse line with a hemagglutinin (HA) tag on the endogenous LHR (HA-LHR) to allow specific immunolocalization of the LHR protein (Baena et al., 2020). The heterogenous expression of the LHR within the mural epithelium allows individual cells to be well visualized (Baena et al., 2020). The mural granulosa region of a mouse preovulatory follicle is comprised of ~5-15 layers of cells, located between the basal lamina and the fluid-filled antrum (Baena and Terasaki, 2019; Baena et al., 2020; Norris et al., 2007; Figures 1A, 2A, S1). Before LHR stimulation, almost all of the LHR-expressing cell bodies in the mural granulosa are located in its outer half, and within this region, expression is heterogeneous (Baena et al., 2020). Many of the LHR-expressing granulosa cells have an elongated flask-like shape, with the cell bodies containing their nuclei located a few cell layers away from the basal lamina and long processes extending back to the basal lamina, forming a pseudostratified epithelium (Baena et al., 2020; Lipner and Cross, 1968; Figures 2A, S1). In the present study, only ~7% of the total LHR-expressing granulosa cell bodies were found in the inner half of the mural granulosa region before LHR stimulation (Figure 3A,B).

At 2 hours after kisspeptin injection (~30 minutes after the peak of the induced LH surge), the percentage of LHR-expressing cell bodies in the inner mural layer had increased to ~21% (Figures 2B, 3B, S2). At later time points after kisspeptin injection, this percentage continued to increase, reaching ~35% at 10 hours (Figures 2C-F, 3B, S3-S6). Ovulation occurred at ~12 hours after kisspeptin (Figures 1B, 2G, S7). Injection with PBS instead of kisspeptin did not change the percentage of LHR-expressing cells in the inner mural granulosa layer at 6 hours, indicating that the localization change is dependent on LH (Figures 3B, S8).

During the 10 hours after kisspeptin injection, there was no change in the percentage of mural granulosa cells expressing HA-LHR protein (Figure 3C). Because studies of rat ovaries have shown that LHR stimulation decreases LHR mRNA and LHR ligand binding in homogenates (LaPolt et al., 1990; Richards et al., 1976; Segaloff et al., 1990; Zheng et al., 2020), the lack of effect of LHR stimulation on the number of granulosa cells expressing the LHR over the 10-hour period after injection of mice with kisspeptin was surprising. Therefore, the HA-LHR protein content of ovaries from mice injected with kisspeptin was assessed by quantitative western blotting. The results indicated the LHR protein levels were unchanged over the 12-hour period after injection (Figure S9). Possible explanations for this apparent difference from previous reports include differences in hormonal stimulation protocols (Zheng et al., 2020) and differences between rats and mice. In addition, it is possible that as previously noted (LaPolt et al., 1990), the observed decrease in LHR ligand binding could be due to internalization of the LHR in granulosa cells (Sposini and Hanyaloglu, 2018) rather than a decrease in total LHR protein.

LH induces an epithelial-to-mesenchymal-like transition in LHR-expressing granulosa cells

High resolution Airyscan images of ovaries from mice before and after kisspeptin injection showed that by 6 hours many LHR-expressing cells in the follicle interior were rounder compared to the predominantly flask-shaped cells seen near the basal lamina prior to LHR stimulation (Figures 3D,E, S10, S11). At 6 hours, many of the LHR-expressing cells had lost a visible attachment to the basal lamina, suggesting that these cells had detached, undergoing an epithelial-to-mesenchymal-like transition (Figures 3E,F, S11). Alternatively, the cellular processes connecting these cell bodies to the basal lamina might have been too thin to see with light microscopy or might not have been contained within the 10 μm thick section. These cells often had numerous filopodia extending in many directions, as well as membrane blebs

173 (Figure 3E,F), consistent with the presence of filopodia and blebs on other migratory cells
174 (Paluch and Raz, 2013; Truszkowski et al., 2023; Xue et al., 2010).
175
176 **LH induces invaginations of the basal lamina and constrictions of the follicle wall**
177 The LH-induced extension of the LHR-expressing granulosa cells into the inner half of the
178 mural layer, and the associated changes in cell shape, raised the question of how these cellular
179 events might correlate with changes in the shape of the follicle as a whole. Labeling of the
180 basal lamina in equatorial sections of follicles in ovaries revealed that follicular shape changes
181 began as early as 6 hours after kisspeptin injection, 6 hours before ovulation (Figures 4, S1B,
182 S4B, S5B, S6B). In follicles in ovaries from mice that had not been injected with kisspeptin, the
183 basal lamina was smooth, with only occasional inward deflections (Figure 4A, C). However, at
184 6-10 hours after kisspeptin injection, the basal lamina showed numerous invaginations, ranging
185 in depth from 5 to 100 μm (Figures 4B-D). The invaginations were localized almost entirely on
186 the basolateral sides of the follicles, and their number increased between 6 and 10 hours after
187 kisspeptin injection (Figure 4E). In addition to the invaginations, equatorial sections of follicles
188 at 8 and 10 hours after kisspeptin injection usually showed large constrictions, where the follicle
189 wall appeared to have contracted on the baso-lateral side (Figures 4C, S5, S6). At 8 hours,
190 many had a concavity on the apical side (Figures 4B, C, S5).
191 Invaginations and constrictions in the follicular wall have been reported previously, in studies
192 of mice, rats, and hamsters (Brown et al., 2010; Gothié, 1967; Ko et al., 2006; Martin and
193 Talbot, 1981; Szołtys et al., 1994; Talbot and Chacon, 1982). Almost all of these previously
194 described shape changes were seen at the time of ovulation or within the hour preceding it,
195 although one study of rats described such shape changes at ~2 hours before ovulation (Szołtys
196 et al., 1994). Our studies indicate that follicular shape changes begin as early as 6 hours before
197 ovulation.
198 The early changes in follicular shape reported here precede the synthesis of endothelin
199 mRNA by the granulosa cells, which is first detected at 11 hours after injection of mice with the
200 LHR agonist hCG (Palanisamy et al., 2006), corresponding to ~1 hour before ovulation (Figure
201 1B). Therefore, endothelin-induced constriction of the follicle mediated by contraction of
202 smooth muscle cells in the theca (Ko et al., 2006; Ko et al., 2022) cannot account for these
203 early changes in follicular shape. The extension of LHR-expressing cells into the basolateral
204 follicle wall could be one of the contributing factors.

205 Investigation of the possible relationship between these invaginations and constrictions and
206 the preceding ingression of LHR-expressing granulosa cells within the follicle could be
207 furthered by knowledge of the cytoskeletal changes that cause the cells to extend, such that
208 the ingression could be inhibited. Notably, activation of the actin severing and depolymerizing
209 protein cofilin is required for LH-stimulated granulosa cell motility in vitro (Karlsson et al., 2010),
210 suggesting a possible function of cofilin in granulosa cell ingression within the follicle in vivo.
211 Cofilin is also essential for other developmental processes involving cellular extension, such
212 as axon growth (Tedeschi et al., 2019). Mice with genetically modified cofilin or other
213 cytoskeletal proteins in their granulosa cells could be used to investigate the cytoskeletal
214 mechanisms that mediate LH-induced granulosa cell ingression in preovulatory follicles, and
215 the consequences for follicular shape changes and ovulation. Acting together with contractile
216 events occurring outside of the basal lamina (Ko et al., 2006; Ko et al., 2022; Migone et al.,
217 2016), LH-induced ingression of LHR-expressing cells within the mural granulosa layer is a
218 new component in the complex sequence of structural changes in the follicle that lead to
219 ovulation.

MATERIALS AND METHODS

Mice

Protocols covering the maintenance and experimental use of mice were approved by the Institutional Animal Care Committee at the University of Connecticut Health Center. Mice with an HA tag on the endogenous LH receptor were as described by Baena et al. (2020); homozygotes were used for all experiments. The HA-LHR and wildtype mouse background was C57BL/6J.

Hormone injections of mice for collection of ovaries and assessment of ovulation

Ovaries containing preovulatory follicles were obtained by injecting 22–24-day-old mice intraperitoneally with 5 I.U. equine chorionic gonadotropin (ProSpec #HOR-272). 44 hours later, the mice were injected with 1 nmol kisspeptin-54 (Cayman Chemical, #24477) to stimulate an endogenous LH surge (Owen et al., 2021). Ovaries were dissected at indicated time points after kisspeptin injection.

To assess ovulation, cumulus-oocyte complexes were collected from oviducts dissected after hormone injections as described above. For figure 1B, some mice were injected with human chorionic gonadotropin (hCG, 5 I.U., ProSpec #HOR-250) instead of kisspeptin. Cumulus-oocyte complexes were dissociated by pipetting and then counted.

Preparation of ovary cryosections for immunofluorescence microscopy

Ovaries were frozen, fixed, cryosectioned, and labelled for immunofluorescence microscopy as previously described (Baena et al., 2020). Sections were 10 μm thick. Antibody sources and concentrations are listed in Table S1. Equatorial sections of follicles, defined as sections including the oocyte, were used for imaging.

Confocal and Airyscan imaging

Ovarian cryosections were imaged with a confocal microscope (LSM800 or LSM980, Carl Zeiss Microscopy). To image entire follicle cross-sections, a 20x/0.8 NA Plan-Apochromat objective was used. Small regions of follicles were imaged using a 63x/1.4 NA Plan-Apochromat objective with an Airyscan detector to enhance resolution. Images of optical sections were reconstructed using the 2-dimensional Airyscan processing at standard strength. Brightness and contrast were adjusted after analysis in Fiji software.

253

254 **Image analysis**

255 To quantify the percentage of HA-LHR expressing cell bodies that were located in the inner
256 half of the mural granulosa layer (Figure 3A,B), inner and outer halves were defined as
257 previously described (Baena et al., 2020). In brief, the width of the mural granulosa layer from
258 antrum to basal lamina was measured at 8 radial positions for each follicle, and halfway points
259 were marked. These points were then connected to define the boundary of the inner and outer
260 mural. The basal lamina position was identified by locating the outer edge of the outermost
261 layer of granulosa cells, or by labeling with an antibody against laminin gamma 1. HA-LHR
262 expressing cell bodies were identified as DAPI-stained nuclei that were surrounded by HA
263 labeling, and were counted in inner and outer mural granulosa cell regions using the Cell
264 Counter Tool in Fiji (Schindelin et al., 2012). The percentage of HA-LHR expressing cells in
265 the inner mural was calculated by dividing the number of HA-LHR expressing cells in the inner
266 mural by the total number of HA-LHR-expressing cells in the inner and outer mural regions.
267 The percentage of mural granulosa cells that expressed the HA-LHR (Figure 3C) was
268 calculated by dividing the total number HA-LHR expressing cells by the total number of DAPI-
269 stained nuclei.

270 Basal lamina invaginations were analyzed using images of equatorial sections in which the
271 basal lamina was labelled with an antibody against laminin gamma 1 (Table S1). Invaginations
272 were defined as regions where the basal lamina curved inwards to a depth of 5-100 μm, with
273 a width of ≤150 μm. The depth of each invagination (Figure 4D) was determined by drawing a
274 line connecting the 2 points on the basal lamina at which it curved inwards, and then measuring
275 the distance between that line and the deepest point of the invagination. For counts of the
276 number of invaginations per cross-section (Figure 4E), the apical region of the follicle was
277 defined as the mural granulosa region adjacent to the surface epithelium. The basolateral
278 region was defined as the rest of the mural granulosa.

279

280 **Western blotting**

281 For measurement of HA-LHR protein content (Figure S9), ovaries were collected at
282 designated time points and sonicated in 1% SDS with protease inhibitors (Norris et al., 2008).
283 Protein concentrations were determined with a BCA assay (Thermo Scientific, #23227) and 40
284 μg of total protein was loaded per lane. Western blots were probed with an antibody against
285 the HA epitope, developed using a fluorescent secondary antibody (Table S1), and detected

286 with an Odyssey imager (LICOR, Lincoln, NE). Blots were co-imaged with the Revert stain for
287 total protein (LICOR), and HA-LHR fluorescence intensity was normalized to the Revert
288 fluorescence intensity for each lane. Values were then normalized to that for the ovary without
289 kisspeptin injection.
290
291 **Statistics**
292 Analyses were conducted as indicated in the figure legends using Prism 9 (GraphPad
293 Software, Inc, La Jolla, CA). All values are presented as mean ± standard error of the mean
294 (SEM).
295

Acknowledgements

We thank Lydia Sorokin and Siegmund Budny for generously providing the laminin antibody, Deb Kaback and Tracy Uliasz for technical assistance, Mark Terasaki, Jeremy Egbert, Rachael Norris, Siu-Pok Yee, Valentina Baena, Tabea Marx, Chris Thomas, and Melina Schuh for helpful discussions, and John Eppig for critical reading of the manuscript.

Competing interests

The authors declare no competing or financial interests.

Funding

This work was supported by the *Eunice Kennedy Shriver* National Institute of Child Health and Human Development (R37 HD014939 to L.A.J., and F31 HD107918 to C.M.O.).

Data availability

All relevant data can be found within the article and its supplementary information.

314 **REFERENCES**

315

316 **Baena, V. and Terasaki, M.** (2019). Three-dimensional organization of transzonal
317 projections and other cytoplasmic extensions in the mouse ovarian follicle. *Sci Rep* **9**,
318 1–13.

319 **Baena, V., Owen, C. M., Uliasz, T. F., Lowther, K. M., Yee, S.-P., Terasaki, M., Egbert, J.
320 R. and Jaffe, L. A.** (2020). Cellular heterogeneity of the luteinizing hormone receptor
321 and its significance for cyclic GMP signaling in mouse preovulatory follicles.
322 *Endocrinology* **161**, bqaa074.

323 **Ben-Ze'ev, A. and Amsterdam, A.** (1989). Regulation of cytoskeletal protein organization
324 and expression in human granulosa cells in response to gonadotropin treatment.
325 *Endocrinology* **124**, 1033–1041.

326 **Bianco, S., Bellefleur, A.-M., Beaulieu, É., Beauparlant, C. J., Bertolin, K., Droit, A.,
327 Schoonjans, K., Murphy, B. D. and Gévry, N.** (2019). The ovulatory signal
328 precipitates LRH-1 transcriptional switching mediated by differential chromatin
329 accessibility. *Cell Reports* **28**, 2443-2454.e4.

330 **Bortolussi, M., Marini, G. and Dal Lago, A.** (1977). Autoradiographic study of the
331 distribution of LH(HCG) receptors in the ovary of untreated and gonadotrophin-primed
332 immature rats. *Cell Tissue Res.* **183**, 329–342.

333 **Bortolussi, M., Marini, G. and Reolon, M. L.** (1979). A histochemical study of the binding of
334 125I-HCG to the rat ovary throughout the estrous cycle. *Cell Tissue Res* **197**, 213–
335 226.

336 **Brown, H. M., Dunning, K. R., Robker, R. L., Boerboom, D., Pritchard, M., Lane, M. and
337 Russell, D. L.** (2010). ADAMTS1 cleavage of versican mediates essential structural
338 remodeling of the ovarian follicle and cumulus-oocyte matrix during ovulation in mice.
339 *Biol Reprod* **83**, 549–557.

340 **Cacioppo, J. A., Lin, P.-C. P., Hannon, P. R., McDougle, D. R., Gal, A. and Ko, C.** (2017).
341 Granulosa cell endothelin-2 expression is fundamental for ovulatory follicle rupture.
342 *Sci Rep* **7**, 817.

343 **Clarke, H. J.** (2022). Transzonal projections: Essential structures mediating intercellular
344 communication in the mammalian ovarian follicle. *Mol Reprod Dev* **89**, 509–525.

345 **Das, D. and Arur, S.** (2022). Regulation of oocyte maturation: Role of conserved ERK
346 signaling. *Mol Reprod Dev* **89**, 353–374.

347 **Downs, S. M. and Longo, F. J.** (1983). An ultrastructural study of preovulatory apical
348 development in mouse ovarian follicles: effects of indomethacin. *The Anatomical*
349 *Record* **205**, 159–168.

350 **Duffy, D. M., Ko, C., Jo, M., Brannstrom, M. and Curry, T. E.** (2019). Ovulation: parallels
351 with inflammatory processes. *Endocrine Reviews* **40**, 369–416.

352 **Eppig, J. J.** (1982). The relationship between cumulus cell-oocyte coupling, oocyte meiotic
353 maturation, and cumulus expansion. *Dev Biol* **89**, 268–272.

354 **Eppig, J. J., Wigglesworth, K. and Pendola, F. L.** (2002). The mammalian oocyte
355 orchestrates the rate of ovarian follicular development. *PNAS* **99**, 2890–2894.

356 **Gothié, S.** (1967). Contribution à l'etude cinétique de l'ovulatoin chez la Souris prépubère. *C*
357 *R Seances Soc Biol Fil* **161**, 554–556.

358 **Grossman, H., Chuderland, D., Ninio-Many, L., Hasky, N., Kaplan-Kraicer, R. and**
359 **Shalgi, R.** (2015). A novel regulatory pathway in granulosa cells, the LH/human
360 chorionic gonadotropin-microRNA-125a-3p-Fyn pathway, is required for ovulation.
361 *The FASEB Journal* **29**, 3206–3216.

362 **Harasimov, K., Uraji, J., Mönnich, E. U., Holubcová, Z., Elder, K., Blayney, M. and**
363 **Schuh, M.** (2023). Actin-driven chromosome clustering facilitates fast and complete
364 chromosome capture in mammalian oocytes. *Nat Cell Biol* **25**, 439–452.

365 **Hughes, C. H. K. and Murphy, B. D.** (2021). Nuclear receptors: Key regulators of somatic
366 cell functions in the ovulatory process. *Molecular Aspects of Medicine* **78**, 100937.

367 **Jaffe, L. A. and Egbert, J. R.** (2017). Regulation of mammalian oocyte meiosis by
368 intercellular communication within the ovarian follicle. *Annu. Rev. Physiol.* **79**, 237–
369 260.

370 **Karlsson, A. B., Maizels, E. T., Flynn, M. P., Jones, J. C., Shelden, E. A., Bamburg, J. R.**
371 **and Hunzicker-Dunn, M.** (2010). Luteinizing hormone receptor-stimulated
372 progesterone production by preovulatory granulosa cells requires protein kinase A-
373 dependent activation/dephosphorylation of the actin dynamizing protein cofilin. *Mol*
374 *Endocrinol* **24**, 1765–1781.

375 **Ko, C., Gieske, M. C., Al-Alem, L., Hahn, Y., Su, W., Gong, M. C., Iglarz, M. and Koo, Y.**
376 (2006). Endothelin-2 in ovarian follicle rupture. *Endocrinology* **147**, 1770–1779.

377 **Ko, C. J., Cho, Y. M., Ham, E., Cacioppo, J. A. and Park, C. J.** (2022). Endothelin 2: a key
378 player in ovulation and fertility. *Reproduction* **163**, R71–R80.

379 **LaPolt, P. S., Oikawa, M., Jia, X. C., Dargan, C. and Hsueh, A. J.** (1990). Gonadotropin-
380 induced up- and down-regulation of rat ovarian LH receptor message levels during
381 follicular growth, ovulation and luteinization. *Endocrinology* **126**, 3277–3279.

382 **Lecuit, T. and Lenne, P.-F.** (2007). Cell surface mechanics and the control of cell shape,
383 tissue patterns and morphogenesis. *Nat Rev Mol Cell Biol* **8**, 633–644.

384 **Lipner, H. and Cross, N. L.** (1968). Morphology of the membrana granulosa of the ovarian
385 follicle. *Endocrinology* **82**, 638–641.

386 **Liu, X., Xie, F., Zamah, A. M., Cao, B. and Conti, M.** (2014). Multiple pathways mediate
387 luteinizing hormone regulation of cGMP signaling in the mouse ovarian follicle. *Biol*
388 *Reprod* **91**, 9.

389 **Martin, G. G. and Talbot, P.** (1981). The role of follicular smooth muscle cells in hamster
390 ovulation. *J Exp Zool* **216**, 469–482.

391 **Martin, G. G. and Talbot, P.** (1987). Formation of the rupture site in preovulatory hamster
392 follicles: morphological and morphometric analysis of thinning of the granulosa and
393 thecal layers. *Gamete Res* **17**, 303–320.

394 **Migone, F. F., Cowan, R. G., Williams, R. M., Gorse, K. J., Zipfel, W. R. and Quirk, S. M.**
395 (2016). In vivo imaging reveals an essential role of vasoconstriction in rupture of the
396 ovarian follicle at ovulation. *Proc Natl Acad Sci U S A* **113**, 2294–2299.

397 **Norris, R. P., Freudzon, L., Freudzon, M., Hand, A. R., Mehlmann, L. M. and Jaffe, L. A.**
398 (2007). A Gs-linked receptor maintains meiotic arrest in mouse oocytes, but
399 luteinizing hormone does not cause meiotic resumption by terminating receptor-Gs
400 signaling. *Dev Biol* **310**, 240–249.

401 **Norris, R. P., Freudzon, M., Mehlmann, L. M., Cowan, A. E., Simon, A. M., Paul, D. L.,**
402 **Lampe, P. D. and Jaffe, L. A.** (2008). Luteinizing hormone causes MAP kinase-
403 dependent phosphorylation and closure of connexin 43 gap junctions in mouse
404 ovarian follicles: one of two paths to meiotic resumption. *Development* **135**, 3229–
405 3238.

406 **Owen, C. M., Zhou, X., Bernard, D. J. and Jaffe, L. A.** (2021). Kisspeptin-54 injection
407 induces a physiological luteinizing hormone surge and ovulation in mice. *Biology of*
408 *Reproduction* **104**, 1181–1183.

409 **Palanisamy, G. S., Cheon, Y.-P., Kim, J., Kannan, A., Li, Q., Sato, M., Mantena, S. R.,**
410 **Sitruk-Ware, R. L., Bagchi, M. K. and Bagchi, I. C.** (2006). A novel pathway
411 involving progesterone receptor, endothelin-2, and endothelin receptor B controls
412 ovulation in mice. *Mol Endocrinol* **20**, 2784–2795.

413 **Paluch, E. K. and Raz, E.** (2013). The role and regulation of blebs in cell migration. *Curr*
414 *Opin Cell Biol* **25**, 582–590.

415 **Parsons, T. T., Mosallaei, S. and Raftery, L. A.** (2023). Two phases for centripetal
416 migration of Drosophila melanogaster follicle cells: initial ingression followed by
417 epithelial migration. *Development* **150**, dev200492.

418 **Peng, X.-R., Hsueh, A. J. W., Lapolt, P. S., Bjersing, L. and Ny, T.** (1991). Localization of
419 luteinizing hormone receptor messenger ribonucleic acid expression in ovarian cell
420 types during follicle development and ovulation. *Endocrinology* **129**, 3200–3207.

421 **Richards, J. S. and Ascoli, M.** (2018). Endocrine, paracrine, and autocrine signaling
422 pathways that regulate ovulation. *Trends Endocrinol Metab* **29**, 313–325.

423 **Richards, J. S., Ireland, J. J., Rao, M. C., Bernath, G. A., Midgley, A. R. and Reichert, L.**
424 **E.** (1976). Ovarian follicular development in the rat: hormone receptor regulation by
425 estradiol, follicle stimulating hormone and luteinizing hormone. *Endocrinology* **99**,
426 1562–1570.

427 **Richards, J. S., Ren, Y. A., Candelaria, N., Adams, J. E. and Rajkovic, A.** (2018). Ovarian
428 follicular theca cell recruitment, differentiation, and impact on fertility: 2017 update.
429 *Endocr Rev* **39**, 1–20.

430 **Schindelin, J., Arganda-Carreras, I., Frise, E., Kaynig, V., Longair, M., Pietzsch, T.,**
431 **Preibisch, S., Rueden, C., Saalfeld, S., Schmid, B., et al.** (2012). Fiji - an Open
432 Source platform for biological image analysis. *Nat Methods* **9**, 10.1038/nmeth.2019.

433 **Segaloff, D. L., Wang, H. Y. and Richards, J. S.** (1990). Hormonal regulation of luteinizing
434 hormone/chorionic gonadotropin receptor mRNA in rat ovarian cells during follicular
435 development and luteinization. *Mol Endocrinol* **4**, 1856–1865.

436 **Sposini, S. and Hanyaloglu, A. C.** (2018). Driving gonadotrophin hormone receptor
437 signalling: the role of membrane trafficking. *Reproduction* **156**, R195–R208.

438 **Stevenson, H., Bartram, S., Charalambides, M. M., Murthy, S., Petitt, T., Pradeep, A.,**
439 **Vineall, O., Abaraonye, I., Lancaster, A., Koysombat, K., et al.** (2022). Kisspeptin-
440 neuron control of LH pulsatility and ovulation. *Front Endocrinol (Lausanne)* **13**,
441 951938.

442 **Stocco, C., Telleria, C. and Gibori, G.** (2007). The molecular control of corpus luteum
443 formation, function, and regression. *Endocrine Reviews* **28**, 117–149.

Szołtys, M., Galas, J., Jabłonka, A. and Tabarowski, Z. (1994). Some morphological and hormonal aspects of ovulation and superovulation in the rat. *J Endocrinol* **141**, 91–100.

Talbot, P. and Chacon, R. S. (1982). In vitro ovulation of hamster oocytes depends on contraction of follicular smooth muscle cells. *J Exp Zool* **224**, 409–415.

Tedeschi, A., Dupraz, S., Curcio, M., Laskowski, C. J., Schaffran, B., Flynn, K. C., Santos, T. E., Stern, S., Hilton, B. J., Larson, M. J. E., et al. (2019). ADF/Cofilin-Mediated Actin Turnover Promotes Axon Regeneration in the Adult CNS. *Neuron* **103**, 1073-1085.e6.

Truszkowski, L., Batur, D., Long, H., Tarbashevich, K., Vos, B. E., Trappmann, B. and Raz, E. (2023). Primordial germ cells adjust their protrusion type while migrating in different tissue contexts in vivo. *Development* **150**, dev200603.

Uilenbroek, J. T. and Richards, J. S. (1979). Ovarian follicular development during the rat estrous cycle: gonadotropin receptors and follicular responsiveness. *Biol Reprod* **20**, 1159–1165.

Walck-Shannon, E. and Hardin, J. (2014). Cell intercalation from top to bottom. *Nat Rev Mol Cell Biol* **15**, 34–48.

Xue, F., Janzen, D. M. and Knecht, D. A. (2010). Contribution of filopodia to cell migration: a mechanical link between protrusion and contraction. *Int J Cell Biol* **2010**, 507821.

Zheng, C., Gulappa, T., Menon, B. and Menon, K. M. J. (2020). Association between LH receptor regulation and ovarian hyperstimulation syndrome in a rodent model. *Reproduction* **160**, 239–245.

468 **FIGURE LEGENDS**

469 **Figure 1. Follicle organization, time course of kisspeptin-induced ovulation, and**
470 **experimental design.** A) Tissue layers of a preovulatory mouse follicle. B) Time course of
471 kisspeptin-induced ovulation in wild-type and HA-LHR-expressing mice. The time course of
472 hCG-induced ovulation in wild-type mice is shown for comparison. Oviducts were collected at
473 the indicated time points, and the numbers of ovulated oocytes were counted (n= 3 mice per
474 each condition). C) Collection of ovaries after kisspeptin injection, for analysis of the
475 localization of HA-LHR-expressing cells by confocal microscopy. KP = kisspeptin. Figures A
476 and C were generated in BioRender.com.
477
478 **Figure 2. LH induces inward extension of LHR-expressing cells within the preovulatory**
479 **follicle.** A-G) Confocal images of representative 10 μm thick equatorial cryosections of
480 follicles in ovaries before and 2-12 after injection of HA-LHR-expressing mice with kisspeptin.
481 The sections were labelled for HA immunofluorescence (green), and nuclei were labelled with
482 DAPI (blue). Each panel shows a maximum projection of a stack of 10 optical sections
483 imaged at 1 μm intervals with a 20x/0.8 NA objective. Scale bars = 100 μm. F and G were
484 captured using a lower zoom than the other images to account for increased follicle size.
485
486 **Figure 3. LH induces ingression of LHR-expressing cells and an epithelial-**
487 **mesenchymal-like transition.** A) Schematic of ingression of LHR-expressing cells within the
488 follicle. B) Time course of the increase in the percentage of HA-LHR-expressing cell bodies in
489 the inner half of the mural granulosa region after kisspeptin injection. No change in the
490 distribution of HA-LHR expressing cells was seen at 6 hours after a control injection of PBS.
491 C) No effect of kisspeptin on the percentage of mural granulosa cells that express the HA-
492 LHR. Measurements in B and C were made from images in supplemental figures S1-S6, and
493 S8. For each time point after kisspeptin, 1100-3000 cells from each of 7-14 follicles from 3-7
494 mice were analyzed. Each point on the graphs represents an individual follicle, and bars
495 indicate mean ± SEM. Data were analyzed via one-way ANOVA with the Holm-Sidak
496 correction for multiple comparisons (****$P < 0.0001$). The percent of HA-LHR expressing cells
497 in the inner mural in the 6 hour PBS treatment was significantly different from all treatments
498 except 0 hr. There were no significant differences among time points for data in C. D,E)
499 Images of representative 10 μm thick equatorial cryosections of preovulatory follicles in

500 ovaries from HA-LHR-expressing mice before (D) or 6 hours after kisspeptin injection (E).
501 Each panel shows a maximum projection of a stack of 10 x 1 μm optical sections taken with a
502 63x/1.4 NA objective using the Airyscan detector. Scale bars = 10 μm. F) Filopodia and
503 blebbing observed at the 6-hour time point. Images are maximum projections of a stack of 30
504 x 0.69 μm optical sections taken with 63x/1.4 NA objective using the Airyscan detector. Scale
505 bar = 5 μm.
506
507 **Figure 4. LH induces basal lamina invaginations and constrictions in the basolateral**
508 **region of the follicle.** A,B) Representative images of follicles before kisspeptin injection (A)
509 and 8 hours afterwards (B), labeled for laminin gamma 1 (white). Scale bars = 100 μm. C)
510 Tracings of the basal lamina of follicles in equatorial sections at 0, 6, 8, or 10 hours after
511 kisspeptin injection (from images in Figures S1B, S4B, S5B, S6B). The tracings are aligned
512 such that the apical region is on the right, as indicated by the double line. Apical was defined
513 as the region that is directly adjacent to the surface epithelium, while basolateral was defined
514 as any portion of the follicle that is not in contact with the surface epithelium. Scale bar = 100
515 μm. D) Depth of invaginations in follicles at 0, 6, 8, and 10 hr post kisspeptin. Each symbol
516 represents one invagination. E) Total number of invaginations in apical and basolateral
517 regions of follicles at 0, 6, 8, and 10 hr post kisspeptin. Each symbol represents one follicle.
518 Data for D and E were generated using datasets in Figures S1B, S4B, S5B, S6B). 6-7
519 follicles from 2-4 mice were analyzed for each time point. Asterisks indicate significant
520 differences (*$P < 0.05$, **$P < 0.01$, ***$P < 0.001$, ****$P < 0.0001$) between groups after two-
521 way ANOVA with the Holm-Sidak correction for multiple comparisons.
522
523
524
525
526
527
528
529
530
531
532

533 Figure 1.

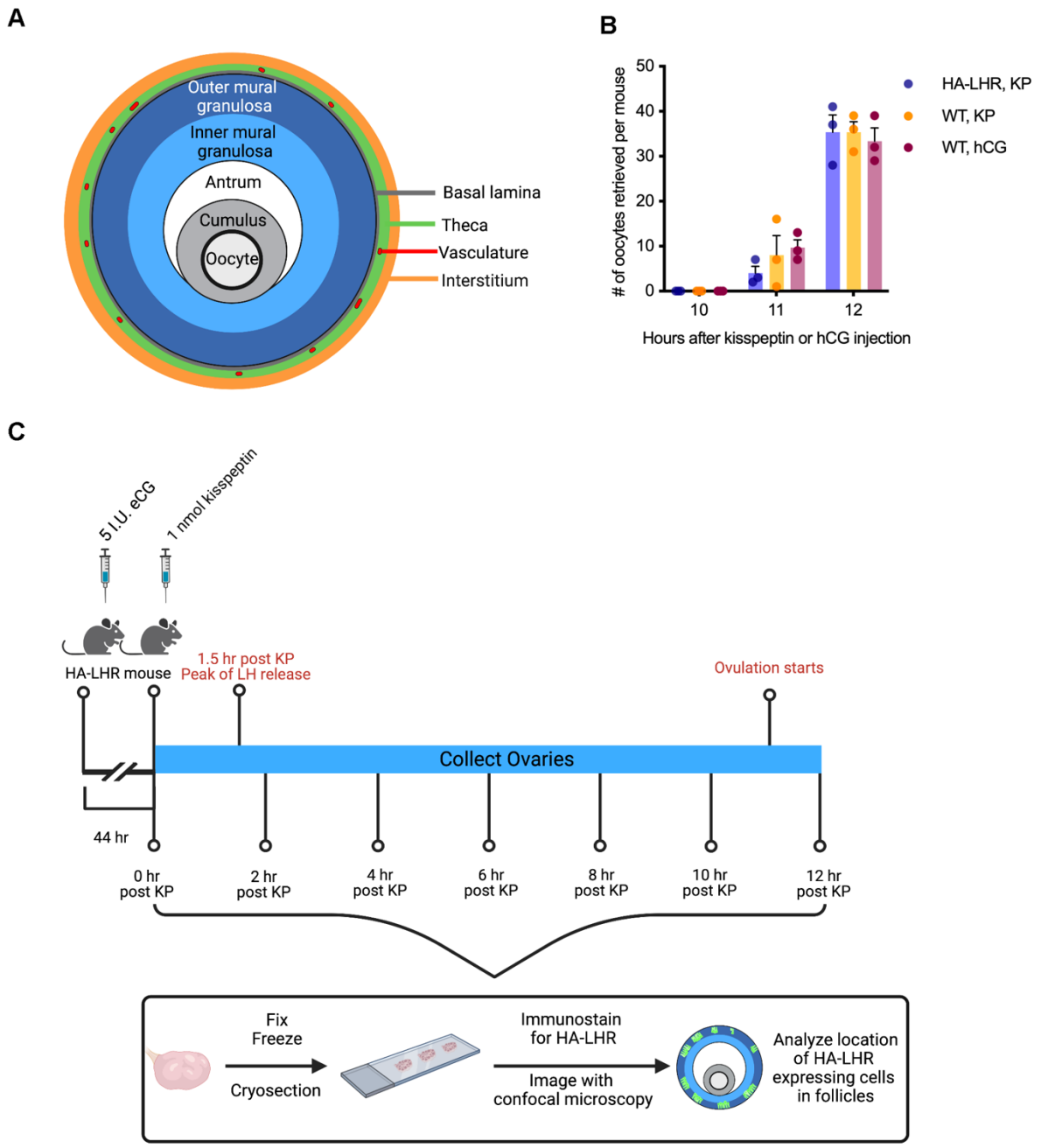

534
535
536
537
538

539 Figure 2.

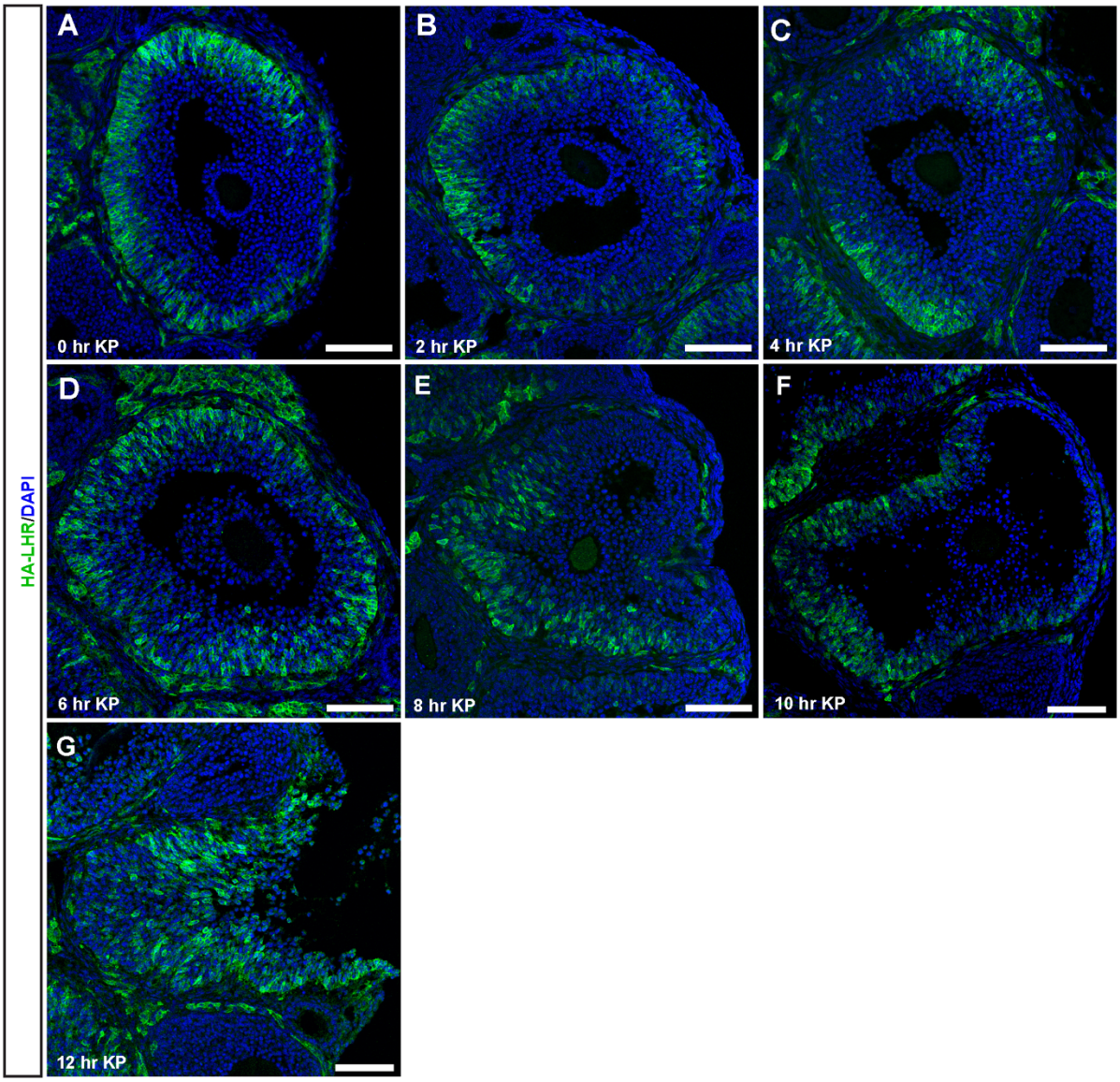

540
541
542
543
544

545 Figure 3.

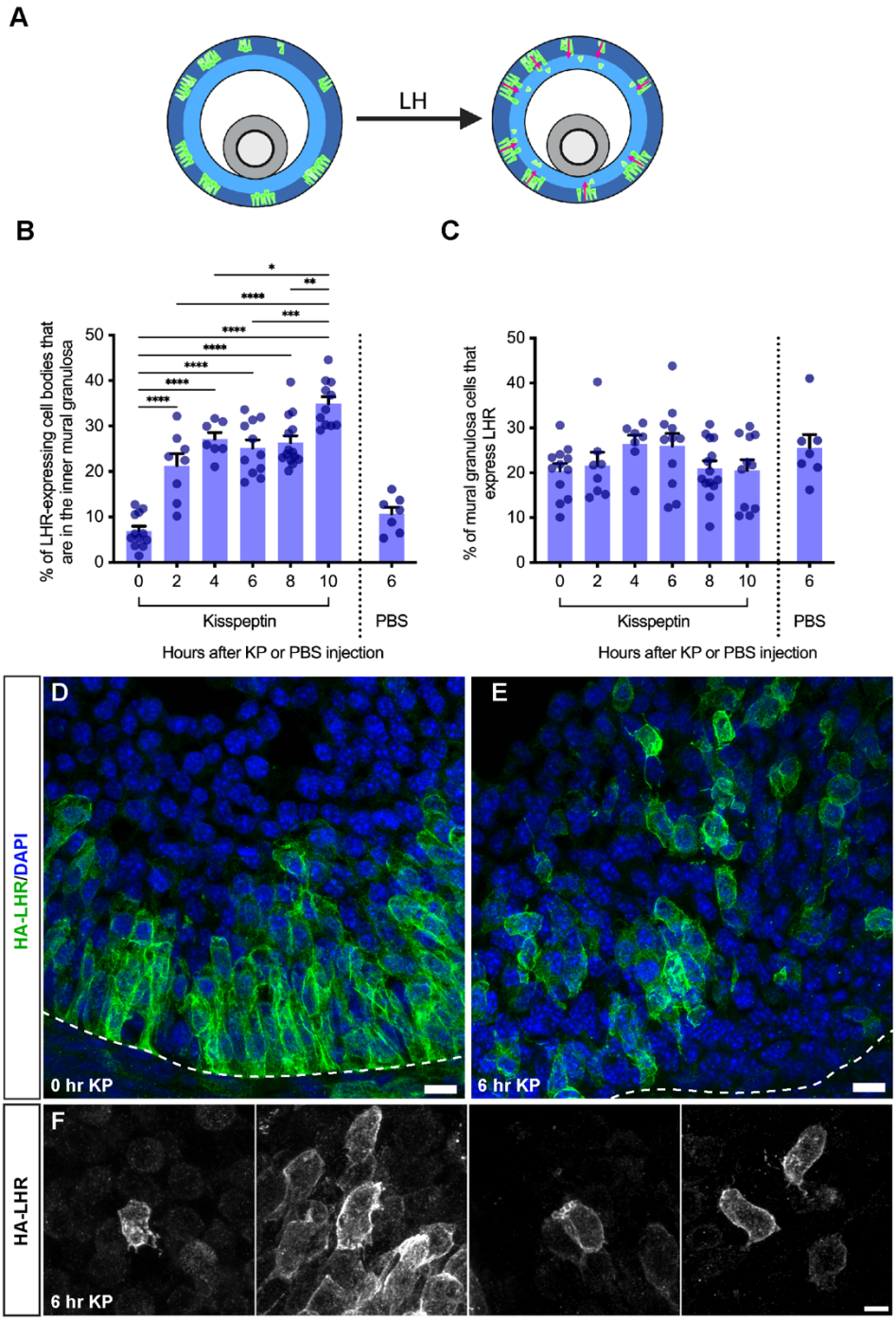

546
547
548
549
550

551 Figure 4.

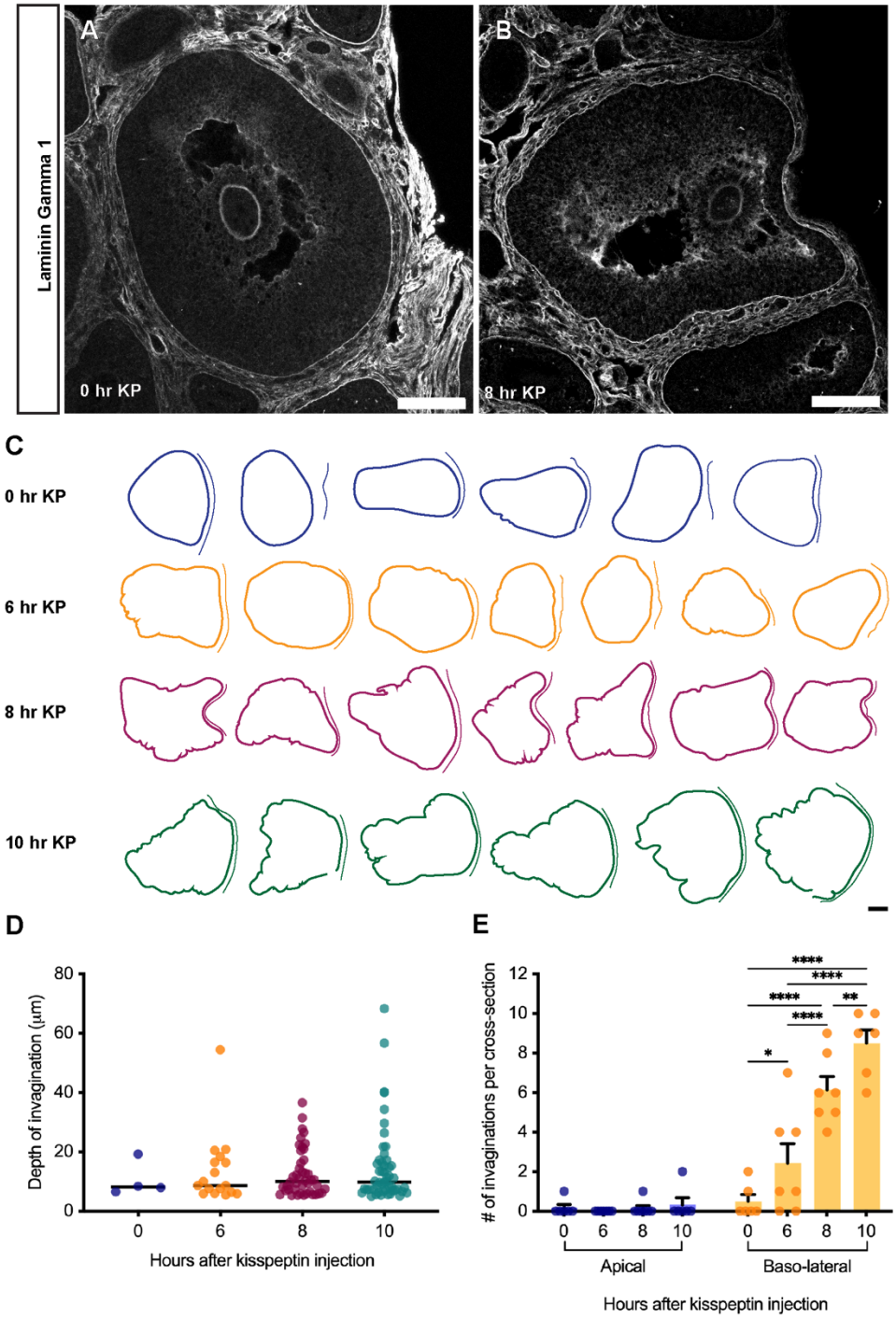

552